J. Phys. D: Appl. Phys. **31** (1998) 671–679. Printed in the UK PII: S0022-3727(98)85829-4

Dynamics of the Levitron™

Roger F Gans†, Thomas B Jones‡ and Masao Washizu§

† Department of Mechanical Engineering, University of Rochester, Rochester, NY 14627, USA
‡ Department of Electrical Engineering, University of Rochester, Rochester, NY 14627, USA
§ Department of Mechanical Engineering, Kyoto University, Sakuo-ku, Kyoto, 606-01 Japan

Received 7 July 1997, in final form 12 November 1997

Abstract. The Levitron™ is an axisymmetric top magnetized parallel to its symmetry axis. It can levitate above a specially constructed magnetic base if spun rapidly enough (and, as we found, not too rapidly). We have written a complete, coupled, nondissipative Hamiltonian system that describes the dynamics of the top. The system is twelfth order and is too complicated for general analysis. We have integrated the equations of motion numerically and found a region of a two-dimensional manifold of initial conditions for which levitation persists. We find that the amplitude of the dynamic variables in the region of persistent levitation scales linearly with the initial tilt of the axis with respect to gravity. We have identified three distinct modes of failure that correspond roughly to insufficient initial spin, too large an initial tilt and too great an initial spin. Our results are in general agreement with published observations and theoretical estimates.

1. Introduction

There have been several papers in the literature recently dealing with the levitating magnetic toy called the Levitron™ (Berry 1996, Jones *et al* 1997, Simon *et al* 1997). The device is a magnetized axisymmetric top that will levitate above a magnetic base if it is spun sufficiently rapidly and carefully. The published work approaches the system with plausible physical approximations about the nature of disturbances to a probably (in the absence of rotation) unstable equilibrium position. The purpose of this paper is to work from first principles, analysing the dynamics without *ad hoc* assumptions. We take a Hamiltonian approach, defining generalized coordinates and their conjugate momenta, and formulating what turns out to be a twelfth-order system. There is one conserved quantity besides the total energy. We find, in common with others, that simple spin about a vertical axis is not sufficient to stabilize the top. We find criteria for the existence of steadily precessing solutions, but these are sufficiently complicated that analytic results regarding stability elude us. We construct a simulation, solving the differential equations numerically, and find that the steady precessing solution is not realized. We do find persistent levitation accompanied by precession and nutation over part of parameter space. We find upper and lower bounds on the permissible rotation rate (actually, the component of total angular momentum parallel to gravity) and the initial nutation angle that allow persistent levitation. We find that the dynamical variables in the region of persistent levitation scale linearly with the initial nutation angle. We identify three distinct modes of failure and approximately where, in parameter space, each occurs. These points are discussed in turn below.

2. Formulation

The kinetic energy of a spinning top is given by the standard formula (see Goldstein (1980) or Meirovitch (1970))

$$T = \tfrac{1}{2}[m(\dot{x}^2+\dot{y}^2+\dot{x}^2)+A(\dot{\theta}^2+\dot{\psi}^2\sin^2\theta)+C(\dot{\phi}+\dot{\psi}\cos\theta)^2] \tag{1}$$

where A and C denote the transverse and polar moments of inertia, m the mass of the top, x, y and z the Cartesian coordinates of the centre of mass of the top with respect to a coordinate system fixed in space (gravity pointing in the negative z direction), and the three angles θ, ψ and ϕ denote the tilt, precession and spin angles respectively (the latter two symbols interchanged from those used by Goldstein). The overdot is used to indicate the derivative with respect to time. The potential energy has two parts, the usual gravitational energy depending on the vertical coordinate of the centre of mass of the top, and a magnetic term obtained by integrating the magnetic moment of the top over the field. We assume the top to be sufficiently small that the integral is unnecessary. The result is

$$V = mgz - M\left[\sin\theta\left(\cos\psi\frac{\partial\Psi}{\partial x}+\sin\psi\frac{\partial\Psi}{\partial y}\right)+\cos\theta\frac{\partial\Psi}{\partial z}\right] \tag{2}$$

where g denotes the acceleration of gravity, M the magnetic moment of the top, supposed to be aligned with the symmetry (spin) axis and Ψ the magnetostatic potential of

the magnetic base. The behaviour of the system seems to be insensitive to the details of the base potential. The base is a plane magnetized perpendicular to its surface with a centred hole or demagnetized volume, and we choose to approximate it by a ring dipole, the potential for which we expand near the axis as

$$\Psi = \frac{M_e}{4\pi R^2}\{f_0(Z) + (X^2+Y^2)f_2(Z) + O[(X^2+Y^2)^2]\} = \frac{M_e}{4\pi R^2}\Phi \tag{3}$$

where M_e denotes the net strength of the ring dipole, R is its effective radius and

$$f_0 = \frac{Z}{(1+Z^2)^{3/2}} \qquad f_2 = -\frac{3}{4}\frac{(2Z^2-3)Z}{(1+Z^2)^{7/2}}.$$

(We have looked at Berry's plate with a hole model, and at a square ring dipole and there is no qualitative difference near the axis.) We have introduced the first part of a nondimensionalization, scaling lengths by R, i.e.

$$x = RX \qquad y = RY \qquad z = RZ \tag{4}$$

and introducing a dimensionless magnetostatic potential Φ. We have examined the potential expansion out through r^6 and find that there is no significant difference (less than 0.05%) in either the vertical or radial field for $r < 0.1$, which is larger than one expects for persistent levitation. We retain the r^2 term to provide a radial field and use the two-term truncation for the rest of this paper. Any truncation error will be swamped by other approximations.

We finish the nondimensionalization by measuring mass in units of m and energy in units of mgR. The consistent time scale is $\sqrt{(R/g)}$, the time it would take the top to fall a distance $R/2$. (For our model of the Levitron™ $R = 34.7$ mm and the time scale is 59.5 ms.) The dimensionless Lagrangian may then be written

$$\mathcal{L} = \tfrac{1}{2}[\dot X^2 + \dot Y^2 + \dot Z^2 + a(\dot\theta^2 + \dot\psi^2\sin^2\theta) + c(\dot\phi + \dot\psi\cos\theta)^2] + \mathcal{M}\left[\sin\theta\left(\cos\psi\frac{\partial\Phi}{\partial X} + \sin\psi\frac{\partial\Phi}{\partial Y}\right) + \cos\theta\frac{\partial\Phi}{\partial Z}\right] - Z \tag{5}$$

where

$$a = \frac{A}{mR^2} \qquad c = \frac{C}{mR^2} \qquad \mathcal{M} = \frac{MM_e}{4\pi mgR^4} \tag{6}$$

are dimensionless numbers characterizing the system. The first two are inertial parameters and the third the ratio of magnetic to gravitational energy.

It is convenient to formulate Hamilton's equations of motion to take advantage of the one cyclic coordinate (ϕ). To that end we choose the generalized coordinates q_i given by the components of the vector $\boldsymbol{q}$

$$\boldsymbol{q} = (X, Y, Z, \theta, \psi, \phi)^{\mathrm{T}} \tag{7}$$

where the superscript T is used to denote the transpose. The conjugate momenta, p_i, are defined by differentiating the Lagrangian with respect to the corresponding generalized coordinate, and the result, in terms of the components of a vector $\boldsymbol{p}$ is

$$\boldsymbol{p} = [\dot X, \dot Y, \dot Z, a\dot\theta, \dot\psi(a\sin^2\theta + c\cos^2\theta) + c\dot\phi\cos\theta, c(\dot\phi + \dot\psi\cos\theta)]^{\mathrm{T}}. \tag{8}$$

We substitute for the physical variables and eliminate the derivatives of the generalized coordinates in terms of the conjugate momenta

$$\dot{\boldsymbol{q}} = \left(p_1, p_2, p_3, \frac{p_4}{a}, \frac{p_5 - p_6\cos q_4}{a\sin^2 q_4}, \frac{p_6[\cos^2 q_4 + (a/c)\sin^2 q_4] - p_5\cos q_4}{a\sin^2 q_4}\right)^{\mathrm{T}}. \tag{9}$$

We can then write the Hamiltonian $\mathcal{H} = \boldsymbol{q}^{\mathrm{T}}\boldsymbol{p} - \mathcal{L}$, which is also the total energy and is conserved, and write Hamilton's equations of motion as

$$\dot{\boldsymbol{q}} = \frac{\partial\mathcal{H}}{\partial\boldsymbol{p}} \qquad \dot{\boldsymbol{p}} = -\frac{\partial\mathcal{H}}{\partial\boldsymbol{q}} \tag{10}$$

where $\mathcal{H}$ is given by

$$\mathcal{H} = \frac{1}{2}\left(p_1^2 + p_2^2 + p_3^2 + \frac{p_4^2}{a} + \frac{[p_5 - p_6\cos(q_4)]^2}{a\sin^2 q_4} + \frac{p_6^2}{c}\right) - \mathcal{M}\left[\sin q_4\left(\cos q_5\frac{\partial\Phi}{\partial q_1} + \sin q_5\frac{\partial\Phi}{\partial q_2}\right) + \cos q_4\frac{\partial\Phi}{\partial q_3}\right] + q_3. \tag{11}$$

Equation (9) gives the explicit evolution for $\boldsymbol{q}$; the evolution equations for $\boldsymbol{p}$ are quite complicated in general. There seems little point in writing them out in their full generality. Note, however, that p_6 is constant.

The trivial solution

$$\boldsymbol{q} = (0, 0, h, 0, \Omega t, \omega t)^{\mathrm{T}} \qquad \boldsymbol{p} = (0, 0, 0, 0, \Omega, \omega)^{\mathrm{T}} \tag{12}$$

satisfies the equations for any values of ω and Ω if

$$\mathcal{M} > \frac{\sqrt{30}}{2880}\frac{(10+\sqrt{30})^{7/2}}{(6+\sqrt{30})^{1/2}} = 8.1880$$

and h takes one of two specific real values, solutions to

$$\frac{3\mathcal{M}h(2h^2-3)}{(1+h^2)^{7/2}} = 1. \tag{13}$$

This solution is unstable to vertical motions if h is equal to the smaller solution and unstable to horizontal motions if h is equal to the larger solution. The two solutions coincide at the minimum value of $\mathcal{M}$, where $h = 1.693\,848\,849\ldots$. This simple instability determined by vertical position agrees with the previous work cited. (The actual numbers depend on the specific choice of base magnetostatic potential function and so will vary with the choice of the base plate model.)

3. Steady precession

The simple solution of erect (parallel to gravity) spin at the height h is unstable. The next simplest solution is that of

steady precession, for which the components of the vectors $\boldsymbol{q}$ and $\boldsymbol{p}$ may be written explicitly as

$$\boldsymbol{q} = (r\cos\Omega t, r\sin\Omega t, h, \alpha, \Omega t, \omega t)^{\mathrm{T}}$$
$$\boldsymbol{p} = [-r\Omega\sin\Omega t, r\Omega\cos\Omega t, 0, 0, \Omega(a\sin^2\alpha + c\cos^2\alpha) + c\omega\cos\alpha, c(\omega+\Omega\cos\alpha)]^{\mathrm{T}} \quad (14)$$

where one is at liberty to choose ω and the r, α, h and Ω must be found to assure that (14) indeed satisfies the equations of motion. Observations of the device suggest that r and α will be small.

The evolution equations for $\boldsymbol{q}$ are automatically satisfied for the choice (14), as is the fifth $\boldsymbol{p}$ evolution equation. The first two evolution equations for $\boldsymbol{p}$ are satisfied if

$$r = 3\frac{\mathcal{M}h\sin\alpha(1+h^2)(h^2-3)}{(12h^4-63h^2+9)\mathcal{M}\cos\alpha + 2(1+h^2)^{9/2}\Omega^2} \quad (15)$$

which is guaranteed to be positive if

$$\left(\frac{21-\sqrt{393}}{8}\right)^{1/2} = 0.3834 < h < \sqrt{3} \quad (16)$$

and Ω^2 does not exceed $-\mathcal{M}\cos\alpha(12h^4-63h^2+9)/2(1+h^2)^{9/2}$. (In this range the numerator of (15) is negative, as is the first factor in the denominator.) As vertical equilibrium is not affected by the addition of precession, we find that h must lie in a very narrow range

$$1.693\,848\,849\ldots < h < \sqrt{3} = 1.732\,050\,808\ldots \quad (17)$$

with the lower limit defined by vertical stability and the upper by equation (16). This is consistent with the observation that the actual top shows persistent levitation in a narrow range of elevation. The third $\boldsymbol{p}$ evolution equation can be satisfied by a correction of $O(\alpha^2)$ to the equilibrium h found in the previous section. The full formula is quite lengthy. We will discuss the essentials later. In any case we cannot have h outside the range defined by (17). Given that the change in h is small, the static equilibrium position also limits $\mathcal{M}$

$$8.187\,957\,439\ldots < \mathcal{M} < 8.211\,203\,828\ldots \quad (18)$$

At $h = 1.72$ and $\mathcal{M} = 8.20$ the upper bound on Ω^2 is $0.779\,296\,7\ldots$.

The fourth $\boldsymbol{p}$ evolution equation, proportional to $\sin\alpha$, determines a relation between Ω and ω. The leading term in an expansion in powers of α is an eighth-degree polynomial in Ω divided by a sixth-degree polynomial in Ω. However, if one assumes that relation (13) between $\mathcal{M}$ and h is satisfied, which is consistent with the small α approximation, the expression simplifies to a fourth-degree polynomial divided by a second-degree polynomial. The denominator vanishes at a precession rate independent of the spin

$$\Omega^2 = \Omega_{cr}^2 = -\frac{4h^4-21h^2+3}{4h^5-2h^3-6h} \quad (19)$$

which lies between 0.56 and 0.66 in the range of interest. The numerator can be written out as

$$12h^2(a-c)f_1(h)\Omega^4 - 12\omega ch^2 f_1(h)\Omega^3 + h[6(a-c)f_2(h) + 4f_3(h)]\Omega^2 - 6\omega ch f_2(h)\Omega + f_4(h) = 0 \quad (20)$$

where

$$f_1 = 4h^6 - 8h^4 - 3h^2 + 9$$
$$f_2 = 8h^6 - 54h^4 + 69h^2 - 9$$
$$f_3 = 4h^8 - 9h^4 - 2h^2 + 3$$
$$f_4 = 13h^8 - 16h^6 - 47h^4 + 2h^2 - 6. \quad (21)$$

The general solution to this is unwieldy, but if we introduce the numerical values of a (=0.089) and c (=0.139), equation (20) reduces to a manageable package for symbolic manipulation by Maple (version 5.0.1 Waterloo Maple Software), although the exact solutions for Ω obtained by introducing the rational versions of a and c are much too lengthy to be reproduced here. On the other hand, viewed as an equation determining ω as a function of Ω, the result is simple. We have a second relation between the two spin rates: that p_6 is conserved. Thus, for small α, we have $\omega + \Omega \approx p_6/c$, where p_6 is a constant of the motion related to the original angular momentum of the top. This will be seen to be the key parameter for the simulation work.

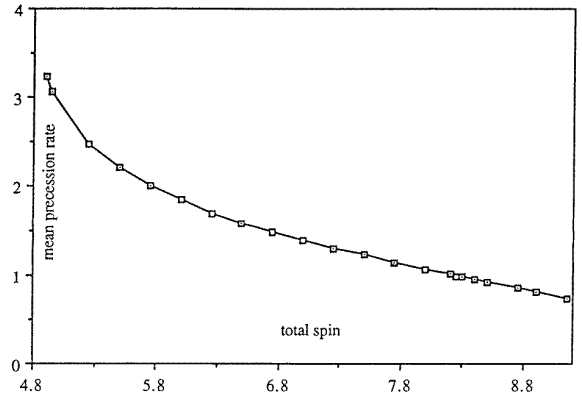

Figure 1. Equilibrium precession rate as a function of total spin in the persistent levitation range.

None of the coefficients are particularly sensitive to h within its limited permissible range, so we set $h = 1.72$. We then equate the two expressions for ω and solve the resulting equation for Ω as a function of p_6. There are four solutions, of which two are complex for moderate values of p_6/c. The other two are real for $0 < p_6/c < 4.8812\ldots$ and complex otherwise. The real values are very insensitive to p_6/c in the range where they exist and may be taken equal to ± 0.77927, their value at $p_6/c = 1$. The spin rate is bounded by $p_6/c + 0.77927$ assuming a positive spin rate and a negative precession rate. The lower bound is then 0.77927 and the upper bound 5.6605. These correspond to spin rates between 125 and 908 rpm, which are lower than the experimentally observed limits, which suggests that the steady precession solutions are unstable and that the experimentally observed state of persistent levitation must have a nutational component. Unfortunately an analytic stability analysis is beyond the scope of this work. It remains to look at the system in simulation, by integrating the equations of motion, and the next section is devoted to that effort.

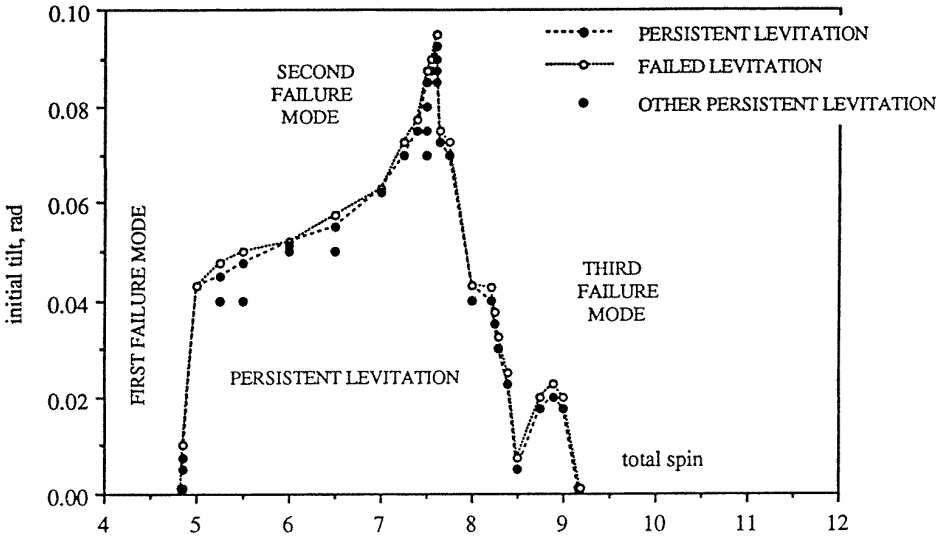

Figure 2. Location of persistent levitation as a function of total spin and initial tilt angle. Failure modes noted on the figure will be discussed below.

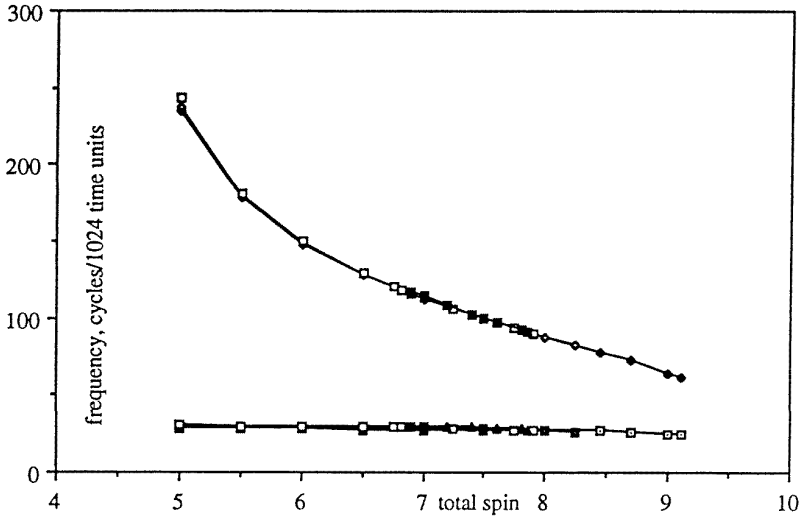

Figure 3. Frequency of radial oscillation as a function of total spin in the persistent levitation regime. Results are superposed for initial tilt angles of 0.015, 0.030, 0.045 and 0.060 radians.

4. Simulations

We have programmed the unrestricted set of equations (10) using the variable step Runge–Kutta routines given by Press *et al* (1992). We integrate adaptively over each of a series of equally long subintervals allowing us to collect data equally spaced in time for later Fourier analysis. We have done considerable numerical experimentation to try to understand the idiosyncrasies of the code. The self-adaptive part of the code makes use of an error measure, comparing the result of two half-interval integrations to a full-interval integration. There is a convergence criterion. We have tested various values of this criterion and find that 10^{-3} is not fine enough, that 10^{-4} is adequate for elapsed times of less than 1000 units (approximately one minute—see below), and that 10^{-5} is good enough for times exceeding 5000 (approximately five minutes). Most of what we report below is based on convergence criteria of either 10^{-4} or 10^{-5}. We will distinguish where it is important.

We fixed the physical parameters $a = 0.089$, $c = 0.139$, $\mathcal{M} = 8.20$ and searched for a restricted range of initial conditions. For these values one time unit is about 59.5 ms; there are about 1000 time units per minute. The code runs three to six times more slowly than real time on a Power Mac 7100/66 at a convergence criterion of 10^{-4}, significantly slower at 10^{-5}. We use the truncated magnetostatic potential of equation (3). We set the initial values of the position of the centre of mass of the system to $(0, 0, 1.72)$, choose the initial phase of ψ and ϕ to be zero and let the velocity of the centre of mass and the tilt angular velocity all be zero. These determine the following initial values for the canonical variables:

$$q_1 = 0 = q_2 \qquad q_3 = 1.72 \qquad q_5 = 0 = q_6$$

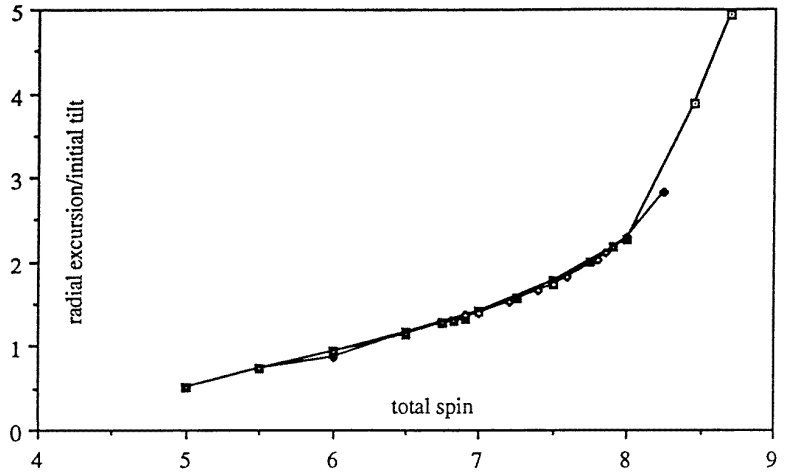

Figure 4. Maximum radial excursion as a function of total spin in the persistent levitation regime. Results are superposed for initial tilt angles of 0.015, 0.030, 0.045 and 0.060 radians.

$$p_1 = 0 = p_2 \qquad p_3 = 0 = p_4. \tag{22}$$

Even within these constraints, there remains a three-dimensional parameter space, and we have uncovered a wide variety of behaviours—more than we can explore thoroughly in this paper. Our objectives are to say something about stability criteria, and to examine the dynamics of persistent levitation and of the transition from levitation to falling. This is an essentially experimental task, and the word stability is used more in a colloquial sense than a technical one. We call the levitating state persistent levitation rather than stable levitation for this reason.

To understand persistent levitation, we need to find conditions under which the device will levitate indefinitely, and conditions under which it will drop out quickly. These are ill-defined words, and we will sharpen our meaning shortly. Apparently we are exploring a three-parameter space of initial conditions, seeking a domain of persistent levitation. The conserved quantity p_6 must be important. It represents the total vertical angular momentum imparted to the top, and is approximately proportional to the square root of its initial kinetic energy. Observations suggest that the tilt angle, $q_4 = \theta$, is small. The equations are singular for zero tilt angle, and the analysis presented above suggests instability in that case, so small initial tilts seem called for. The partition of the rotation associated with p_6 between spin and precession is not obvious for small tilt angles. We ran a number of cases that exhibited persistent levitation, and discovered that the device seeks a specific mean precession rate for each value of p_6. The precession rate jumps from an initial small value (here 0.001) to a value near its long-term average within one time unit for all allowable ω_T. We define a total spin $\omega_T = p_6/c$ and plot the mean precession rate as a function of ω_T in the range of ω_T where persistent levitation is possible in figure 1. The final mean precession rate is a weak function of the initial tilt angle θ_0, increasing with the tilt angle. At $\omega_T = 7.5$ the mean precession (measured by looking at the precession angle after 100 time units) increases from 1.1991 to 1.2278 as θ_0 increases from 0.005 to 0.085. For our simulations we select ω_T and θ_0 and choose the initial value of the precession Ω to be approximately equal to its long-term mean. This reduces, but does not eliminate q_5 and q_6 oscillations: angular momentum is continually exchanged between spin and precession. Thus we are exploring a two-dimensional subspace of the twelve-dimensional $\boldsymbol{q}, \boldsymbol{p}$ space, parameterized by ω_T and θ_0.

Observations of the Levitron™ suggest that the top apparently fails by slowing down and then falling out of equilibrium. On the other hand, the simulation has no mechanism for slowing; when failure occurs, it does so after some interval of time consistent with experimental observations. The time to failure in simulation increases as the initial tilt angle decreases, but not uniformly. One cannot compute for ever, and we need to choose a value beyond which we will call the levitation persistent. We have chosen 1024 time units (about a minute) as a compromise between observations (Simon *et al* (1997) state that levitation can last for more than two minutes; Jones *et al* (1997) state that levitation can last as long as five minutes) and computation time. We have run some examples for longer periods (up to 10 000 time units, in excess of ten minutes). Figure 2 shows a map of stability according to this criterion. Most of the calculations on which the figure is based were done using 10^{-4} as our convergence criterion. We have checked much of the field at 10^{-5} and obtained consistent results. The range of stable total spin is defined by the lower unstable observation at $\omega_T = 4.83$ and an initial tilt of 0.001 radians, and the upper unstable observation of $\omega_T = 9.18$ at the same initial tilt (stable at 4.84 and 9.17 at $\theta_0 = 0.001$ radians). These are well defined: the top becomes rapidly unstable immediately outside the region of persistent levitation at these boundaries.

The motion within the stable region is complicated. There is a vertical oscillation, a radial oscillation, a nutation and an interchange of vertical angular momentum between spin and precession. We have examined these frequencies as a function of ω_T at initial tilts of 0.015, 0.030, 0.045 and 0.060 radians by creating records of 1024 time units

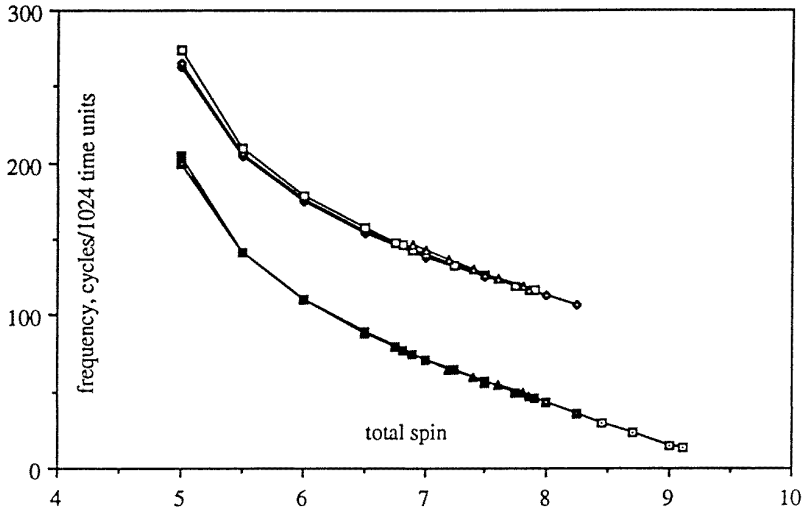

Figure 5. Nutation frequencies as a function of total spin in the persistent levitation regime. Results are superposed for initial tilt angles of 0.015, 0.030, 0.045 and 0.060 radians.

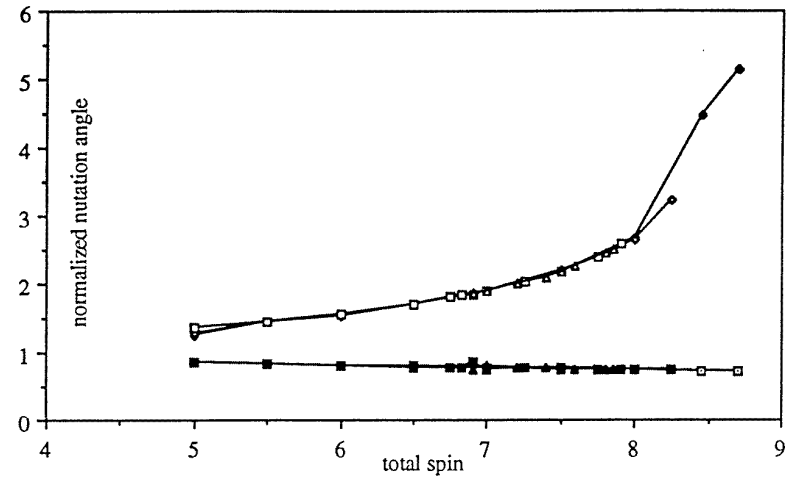

Figure 6. Normalized nutation angle as a function of total spin in the persistent levitation regime. Results are superposed for initial angles of 0.015, 0.030, 0.045 and 0.060 radians.

and 2048 points using 10^{-5} as our convergence criterion, and taking the Fourier transforms of the variables using the Press *et al* (1992) fast Fourier transform (FFT) routines. The power spectra show one to five distinct peaks. We find no signs of chaos in any of the nominal stable systems.

The vertical (Z) oscillation has one dominant frequency. There is also some power at the lowest nutation frequency. The dominant frequency is a weak function of ω_T and of θ_0, increasing with the former and decreasing with the latter. Its value ranges from 25.4 to 28.3 mcptu (millicycles per time unit, a convenient nondimensional unit approximately equal to rev/min). One can calculate a nominal vertical oscillation frequency from the linearized perturbation of the p_3 evolution equation. This is formally independent of spin and precession, depending linearly on $\mathcal{M}$ and $\cos\theta_0$, and nonlinearly on the equilibrium position. The measured frequencies correspond to linear oscillation about an equilibrium position of about 1.701. (The frequency corresponding to the initial value of 1.72 is 50.8 mcptu.) In this range of initial tilt the vertical position remains within one per cent of its initial value.

The X and Y spectra are identical, corresponding to a radial oscillation. (We have specifically examined the behaviour of radius as a function of time, although we do not present the result here.) There are typically three dominant frequencies. One of these is identical to the vertical oscillation frequency. The other two are shown as functions of ω_T in figure 3. We find a high frequency that decreases with spin rate and a lower frequency (not an integer multiple of the Z frequency) that increases slowly with spin. Neither frequency depends on the initial tilt angle θ_0. The amplitude of oscillation is proportional to the initial tilt angle, and increases with increasing spin. Figure 4 shows the maximum radial excursion divided by the initial tilt angle for these stable cases. The data from the four different initial tilt angles fall on the same curve. We take some comfort in the fact that the radial excursions are typically no more than 0.1 (less than 3.5 mm), so that

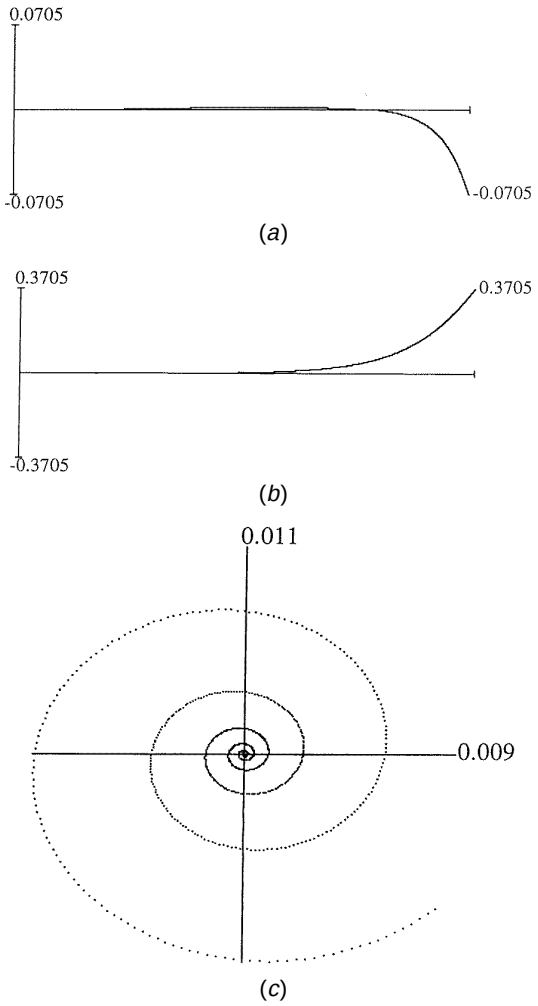

Figure 7. First failure mode: $\omega_T = 4.8$, $\theta_0 = 0.0001$ radians, $\Omega_0 = 3.49$, resolution $= 10^{-5}$, $0 < t < 16.87$. (*a*) δZ versus t, (*b*) θ versus t, (*c*) y versus x phase trajectory.

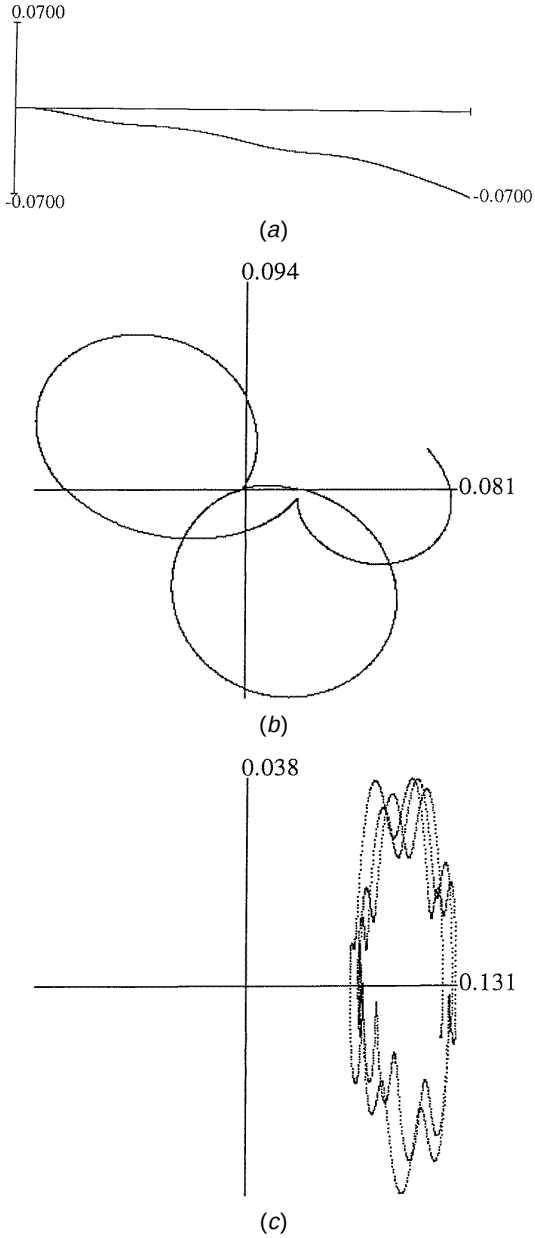

Figure 8. Second failure mode (low range): $\omega_T = 7.0$, $\theta_0 = 0.07$ radians, $\Omega_0 = 1.44$, resolution $= 10^{-5}$, $0 < t < 8.24$. (*a*) δZ versus t, (*b*) y versus x phase trajectory, (*c*) $\dot{\theta}$ versus θ phase trajectory.

neglect of the higher order terms in the potential function is not likely to affect our results.

Figure 5 shows the dominant nutation frequencies. They are identical for all four different initial tilt angles where they have a common range. The nutation frequencies also appear in the spectrum for p_5, showing that they are coupled to the interchange of angular momentum between spin and precession. The maximum and minimum nutation angles, divided by the initial tilt angle, are shown in figure 6. The range of nutation clearly scales with the initial value. Again all four normalized curves are essentially the same.

It is interesting to compare Berry's (1996) qualitative predictions (his section 6) to the results of the simulation. They are remarkably good. We expect different models of the base magnetic field potential to make little qualitative difference. Berry discusses the case that the top is set spinning with an initial spin of 20 Hz. This translates to 7.48 rptu (radians per time unit) in our dimensionless representation. The simulation gives a mean precession rate of 0.94 rptu, which translates to 2.51 Hz, rather close to his adiabatic estimate of 3.8 Hz. The total spin is 8.432, well within the range of stability. We ran an extensive calculation (an elapsed time of 8192 time units, just over eight minutes, recording 4096 fixed data points) of this case at an initial tilt of 0.03 radians using 10^{-5} as our convergence criterion. There are three radial frequencies containing significant power: 0.778, 1.269 and 0.419 Hz. The maximum radial excursion is a little more than 2 mm. There are two vertical frequencies containing significant power: 1.130 and 0.43 Hz. The first compares well with Berry's estimate of 1.4 Hz. The peak to peak vertical excursion is 130 μm, and the mean position is 3 μm below the initial position. There are two dominant nutation frequencies. By far the more important is 0.443 Hz, which also appears in the vertical spectrum. The second is

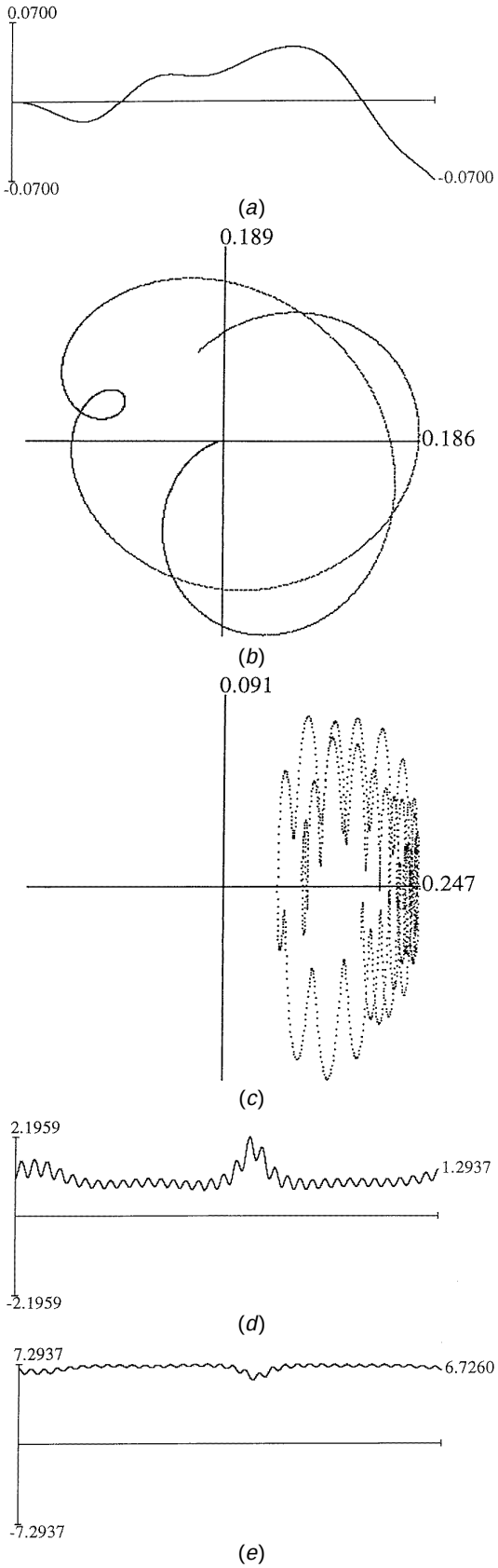

Figure 9. Second failure mode (high range): ω_T = 8.0, θ_0 = 0.10 radians, Ω_0 = 1.04, resolution = 10^{-5}, $0 < t < 20.62$. (*a*) δZ versus t, (*b*) y versus x phase trajectory, (*c*) $\dot{\theta}$ versus θ phase trajectory, (*d*) Ω versus t, (*e*) ω versus t.

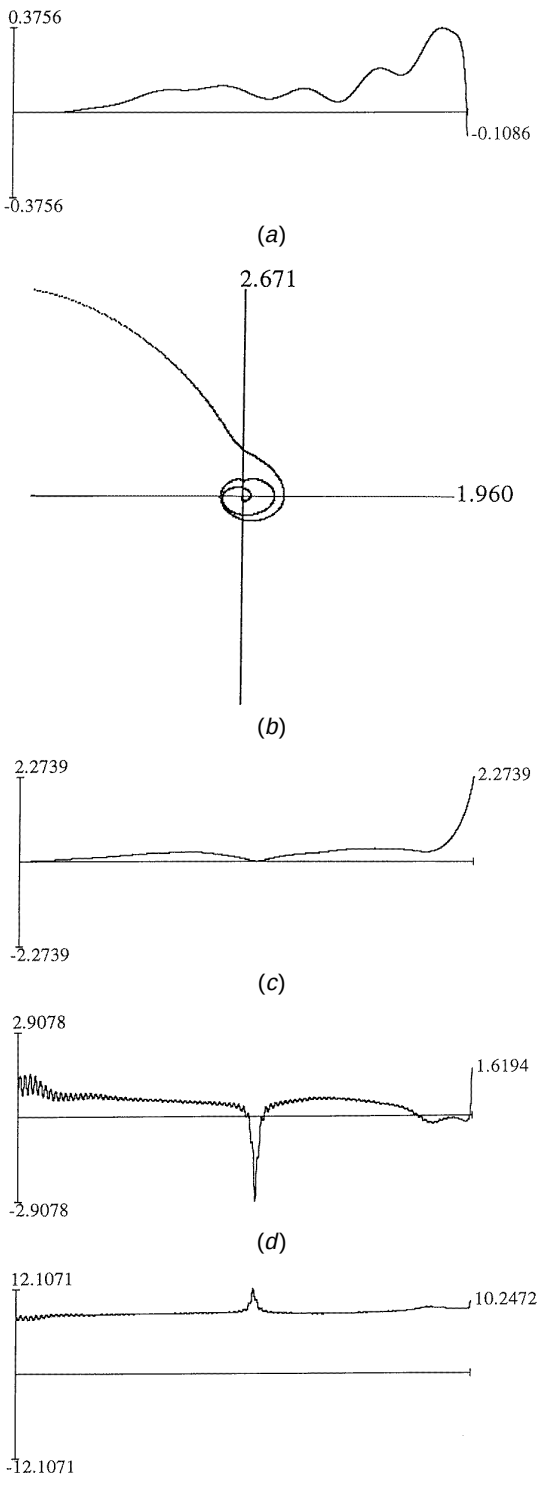

Figure 10. Third failure mode: ω_T = 9.2, θ_0 = 0.025 radians, Ω_0 = 0.72, resolution = 10^{-5}, $0 < t < 45.36$. (*a*) δZ versus t, (*b*) y versus x phase trajectory, (*c*) θ versus t, (*d*) Ω versus t, (*e*) ω versus t.

0.985 Hz. The nutation angle, initially 0.573°, is bounded by 0.410° and 2.097°.

We have examined a number of unstable cases with a view to describing the failure mode, if not the mechanism.

We find three fairly distinct modes of failure that can be located with some precision on the parameter map (figure 2). All of the failure assessments were performed using 10^{-5} as our convergence criterion.

To the left of the zone of persistent levitation ($\omega_T < 4.83$) the top becomes unstable 'explosively', with an apparently exponential increase in tilt angle, radial location of the centre of mass and distance of the centre of mass below its nominal equilibrium position. Figures 7(a)–(c) show the change in vertical location and tilt angle as a function of time, and the location of the centre of mass in the x–y plane during the same time interval respectively for $\omega_T = 4.80$ at an initial tilt angle of 0.0001 radians. The calculation was terminated when the vertical position had dropped from 0.07 to 1.65. This is sufficient to ensure there will be no recovery. The important point to note about this failure mode is the simultaneous growth in all three directions—radial, vertical and nutational. The precession and spin rates oscillate in the early phase of the run, and may be increasing near the end, but the real 'action' is in displacement and tilt. We ran many simulations in this part of the map and find the results to be qualitatively the same. The small quantitative difference do not appear to be meaningful, and we will not discuss them.

The second failure mode occurs when ω_T lies within the persistent levitation range to the left of the peak, but the initial tilt is too high. This failure mode is marked by vertical motions that lead to a dropping of the top without significant change in tilt or radial position. The vertical oscillation is accompanied by nutation and by a complicated motion in the x–y plane. Both are apparently bounded. The amplitude of the motion increases slightly with ω_T. Figures 8(a)–(c) show the vertical motion versus time, the x–y motion during the time interval and a phase plane diagram of the nutation respectively for $\omega_T = 7.00$ at an initial tilt of 0.07 radians. These figures are typical; there is no indication of any secular motions in tilt or in radial location. We also observe nothing remarkable in the spin and precession rates. The same general failure behaviour persists as ω_T increases.

A variation of the second failure mode, observed to the right of the region of persistent levitation is illustrated in figures 9(a)–(e). Figure 9(a) shows the vertical motion, which exhibits a significant rise above equilibrium before the start of the fall. Figures 9(b) and 9(c) show the x–y plane and the tilt phase plane trajectories respectively, and there is nothing remarkable to be noted in either. Figures 9(d) and 9(e), however, show a glitch in the precession and spin rates at about $t = 11$. This behaviour was not noted in any of the simulations discussed so far.

Failure in the third mode, occurring for $\omega_T > 8.4$, is characterized by a leap upward of the centre of mass, accompanied by sharply increasing tilt and radial motion, followed by the usual precipitous drop of the centre of mass. Figures 10(a)–(e) show this behaviour. Figure 10(a) shows the sharp rise in elevation just before the fall. Figure 10(b) shows the rapid lateral excursion of the centre of mass. Figure 10(c) shows the accompanying increase in tilt angle. Finally, figures 10(d) and 10(e) show the same glitch in spin and precession as appears in figures 9(d) and 9(e). Note that this glitch accompanies an approach to zero of the nutation angle. It is not impossible that this approach to a singular condition is connected with the subsequent failure of levitation.

5. Discussion and conclusions

We have shown that the full, nondissipative equations of motion can be used to describe the behaviour of the Levitron™ without any need to make simplifying assumptions. These equations are extremely complicated, even with some simplification of the magnetostatic potential of the base, and do not provide extensive analytical results. Apparently there are no simple solutions that lead to persistent levitation, so that various analytic approaches to stability, such as linearization or nonlinear averaging techniques, already challenged by the sheer dimensionality of the problem, seem unlikely to yield definitive results, restricting the analyst to numerical experimentation.

Simulation is successful, yielding behaviour that is consistent with what experimental observations are available. As such it presents a tool for studying this system, and other systems of high dimensionality and complicated motion. It does not seem important or useful at this point to make the simulation more complicated. The simulation predicts that one can have a short period of apparently persistent levitation followed by rapid failure without the need to introduce any mechanism for slowing the top, or, indeed, any dissipative mechanism at all. We hope that these results can be used as a guide by analysts and experimenters dealing with this and other rotationally constrained problems.

References

Berry M V 1996 The Levitron™: an adiabatic trap for spins *Proc. R. Soc.* A**452** 1207–20

Goldstein H 1980 *Classical Mechanics* 2nd edn (Reading, MA: Addison Wesley)

Jones T B, Washizu M and Gans R F 1997 Simple theory for the Levitron™ *J. Appl. Phys.* **82** 883–8

Meirovitch L 1970 *Methods of Analytical Dynamics* (New York: McGraw-Hill)

Press W H, Teukolsky S A, Vetterling W T and Flannery B P 1992 *Numerical Recipes in C. The Art of Scientific Computing* 2nd edn (Cambridge: Cambridge University Press)

Simon M D, Heflinger L O and Ridgeway S L 1997 Spin stabilized magnetic levitation *Am. J. Phys.* **65** April 286–92